NASA Contractor Report 165717

A CONTROLLER DESIGN APPROACH FOR LARGE FLEXIBLE SPACE STRUCTURES

S. M. Joshi

VIGYAN RESEARCH ASSOCIATES, INC.
Hampton, Virginia 23666

Contract NAS1-16126
May 1981

National Aeronautics and
Space Administration

Langley Research Center
Hampton, Virginia 23665

TABLE OF CONTENTS

SUMMARY

A controller design approach for large space structures is presented, which consists of a primary attitude controller and a secondary or damping-enhancement controller. The secondary controller, which uses several Annular Momentum Control Devices (AMCD's), is shown to make the closed-loop system asymptotically stable under relatively simple conditions. The primary controller using torque actuators (or AMCD's) and colocated attitude and rate sensors is shown to be stable. It is shown that the same AMCD's can be used for simultaneous actuation of primary and secondary controllers. Numerical results are obtained for a large, thin, completely free plate model.

INTRODUCTION

Future utilization of space is expected to require large space structures (LSS) in low Earth and/or geosynchronous orbits. Examples of such future missions include: electronic mail system, Earth observation systems, solar power satellites, and space manufacturing facilities, requiring large antennas, antenna platforms, and solar arrays. These missions will be feasible because of the availability of the space Shuttle for relatively inexpensive transportation into low-Earth orbits. Shuttle capability can be expanded by augmenting a low-Earth to geosynchronous orbit transportation system.

To establish these structures in space at minimum cost will require that their weight be minimized. As a result, these structures will tend to have extremely low-frequency, lightly damped structural modes which are closely-spaced in the frequency domain. Structural parameters (i.e., frequencies,

damping ratios and mode shapes) are usually difficult to determine a priori. For these reasons, control systems design for LSS is a complex and challenging problem. Two types of control systems will be required for LSS: (i) large-angle maneuvering in order to reorient the LSS, and (ii) pointing the LSS in space with the required precision in attitude and shape. The objective of this report is to develop and investigate a controller design methodology for pointing control of LSS.

The basic problems in pointing control of LSS have been well known for several years in the context of control of conventional spacecraft, which are relatively rigid, but which have sufficient flexibility to necessitate consideration in the design process. However, structural flexibility is the most dominant characteristic of LSS, making LSS a new class of spacecraft. Because of pointing requirements it is necessary to have LSS closed-loop rigid-body bandwidth higher than a number of structural mode frequenices. Because of the high order of the LSS state vector (resulting from a large number of dominant structural modes), a practical controller can be designed to actively control only a few of the structural modes. Stability of the system is not assured with low-order controllers, because of control "spillover" (i.e., unwanted forcing of the uncontrolled or "residual" modes by the control input) and observation "spillover" (i.e., unwanted contribution of the residual modes to sensor outputs) (ref. 1). These problems were considered in references 2, 3 and several methods for designing reduced-order controllers based on Linear-Quadratic-Gaussian (LQG) control theory were proposed and discussed in reference 3. Stability of the closed-loop system designed using these methods is heavily

dependent on the inherent damping present in the residual modes (ref. 2). As mentioned previously, inherent damping ratios of residual modes are difficult--if not impossible--to predict. Therefore, it is highly desirable to enhance modal damping of LSS with a robust "secondary" or "damping enhancement" controller. The controller design methodology proposed and investigated in this report takes this approach. The proposed design consists of a two-level control system which includes a primary attitude controller and a robust secondary controller.

Direct velocity feedback controllers (ref. 4) have been proposed in the literature for damping enhancement in LSS. In particular, "member damper" controllers (ref. 5) and low-authority structural controllers (ref. 6) with guaranteed Lyapunov stability, have been proposed. In this report, the use of several Annular Momentum Control Devices (AMCD's) for damping enhancement is proposed and investigated. (See ref. 7 for a description of AMCD.) The secondary controller makes the closed-loop system asymptotically stable under certain relatively simple conditions. Primary attitude controller design is considered using either torque actuators or AMCD's. When the torque actuators are colocated with attitude and rate sensors, the closed-loop system is stable. It is proved that the same AMCD's can be used to accomplish simultaneous primary and secondary controller actuation. The overall control system is shown to be stable for the case when actuators are colocated with sensors. Numerical results are obtained for a large, thin, completely free, flat plate in order to demonstrate and evaluate the controller design methods.

MODEL INVESTIGATION

Mathematical Models of LSS

A large space structure is a highly oscillatory distributed parameter system. A class of large space structures is described by the partial differential equation:

$$A_1\left\{\omega(\delta,t)\right\} + A_2\left\{\frac{\partial}{\partial t}\,\omega(\delta,t)\right\} + m(\delta)\,\frac{\partial^2}{\partial t^2}\,\omega(\delta,t) = f(\delta,t) \qquad (1)$$

where A_1 is a linear operator consisting of partial derivatives of the deflection function $\omega(\delta,t)$ with respect to space variables δ, A_2 is a linear operator describing the inherent structural damping in the LSS, and functions $m(\delta)$ and $f(\delta,t)$ denote the mass distribution and the applied (generalized) force distribution. Assuming zero damping (A_2 = null operator), it is possible to obtain the following normal-coordinate representation using the property of orthogonality of eigenfunctions of A_1, and using appropriate boundary conditions:

$$\ddot{q}_i + \omega_i^2 q_i = \sum_{k=1}^{m} \Phi_{ki} u_k \qquad (i=1,2,\ldots,\infty) \qquad (2)$$

where q_i is the modal amplitude of the ith mode, u_k, k=1,2,...m represent the input which is assumed to consist of generalized point-forces (i.e., forces and moments). Φ_{ki} denotes the value of the ith "mode shape" at the location of kth actuator. The model consists of an infinite number of modes. Since real-life LSS will have some structural damping, a more realistic

representation can be obtained by adding the term $2\rho_i\omega_i$ to the left-hand side of equation (2), where ρ_i and ω_i denote damping ratio and natural frequency of the ith mode. The "observations" or sensor outputs, which consist of position and angular displacements, are given by

$$y_k = \sum_{i=1}^{\infty} \Psi_{ki} q_i \tag{3}$$

where Ψ_{ki} denotes the ith mode-shape evaluated at the location of the kth sensor. The modes in equation (2) also consist of rigid-body modes. It is customary to separate the rigid-body modes from the structural modes, and also to truncate the model at η_e structural modes. For practical LSS, it is usually not possible to analytically obtain the model of the form of equations (1) and (2). The standard technique is to use the finite element method to obtain a model. Established computer programs such as SPAR and NASTRAN are available for this purpose. Finite element structural models also have the same form as the normal-coordinate model (i.e., eqs. (2) and (3)).

For the purpose of this investigation, it was necessary to choose an appropriate model of a LSS as a medium for control law development. After consultation with the NASA technical monitor, a finite element model of a 30.48 m × 30.48 m × 2.54 mm (100 ft × 100 ft × 0.1 in.), completely free aluminum plate was selected for this purpose. This model was developed in reference 8 using the SPAR program. A finite element mesh of 24 × 24 equal square plate elements was used to obtain modal frequencies and mode shapes

(with respect to force and torque inputs)which were computed(ref. 8) for the first 44 modes. Table I gives the rigid-body parameters and the first 44 modal frequencies for this model. Values of the mode-shapes at all 625 nodes are given in reference 8. Rotation about only two axes (x and y axes in fig. 1), and translation in the z-direction were considered in the model since they suffice to demonstrate the principles. Thus the LSS model is given by:

(i) Rigid-body motion:

$$I_s \ddot{\alpha}_s = \sum_{j=1}^{n_T} T_j + \sum_{i=1}^{n_f} R_i \times f_i \qquad (4)$$

$$m_s \ddot{z}_s = \sum_{i=1}^{n_f} f_i \qquad (5)$$

where $\alpha_s = (\phi_s, \theta_s)^T$ denotes the rigid-body attitude vector about x and y axes; z_s denotes z-axis translation of the LSS center of mass; I_s and m_s denote the two-dimensional LSS inertia matrix and LSS mass; f_i and T_j denote applied forces and torques ($i=1,2,..,n_f$; $j=1,2,..,n_T$); R_i denotes the coordinates of point of application of force f_i. It should be noted that the rigid-body translation z_s is not of interest in investigations of the LSS attitude control problem. Equation (5) is included here for completeness, and will be used only in equation (7).

(ii) Flexible motion (assuming no inherent damping)

$$\ddot{q} + \Lambda q = \Phi_f^T f + \Phi_t^T T \tag{6}$$

where q is the n_q-dimensional modal amplitude vector; Λ is a positive definite $n_q \times n_q$ matrix (usually diagonal, with entires = ω_i^2). Φ_f and Φ_t are $n_f \times n_q$ and $n_T \times n_q$ mode shape matrices corresponding to force and torque inputs, and f and T denote vectors consisting of f_i and T_i, respectively.

(iii) Sensor outputs:

Sensed z-axis translation is given by (ignoring noise)

$$z_m = z_s + R_z \times \alpha_s + \phi_f^T q \tag{7}$$

where R_z is the coordinate (vector) of the sensor location, ϕ_f is the $n_{q\times 1}$ mode shape vector at the sensor location. Sensed LSS attitude (ϕ_m, θ_m) is given by

$$\begin{bmatrix} \phi_m \\ \theta_m \end{bmatrix} = \begin{bmatrix} \phi_s \\ \theta_s \end{bmatrix} + \begin{bmatrix} \phi_{tx}^T \\ \phi_{ty}^T \end{bmatrix} q \tag{8}$$

where ϕ_{tx}, ϕ_{ty} are the $n_{q\times 1}$ mode shape vectors at the x and y axis attitude sensor locations.

Controllability and Observability of LSS Model

The LSS variables to be controlled are: rigid-body attitude and rate (α_s and $\dot{\alpha}_s$), and structural modal amplitudes and rates ($q,\dot{q}$). Control inputs are point forces or torques, and observations (sensor outputs) normally consist of an attitude sensor (e.g., sun sensor or star tracker), and an attitude rate sensor (e.g., rate gyro). Let λ_i ($i=1,2,\ldots,n_q$) denote the ith eigenvalue of Λ ($\lambda_i = \omega_i^2$ where ω_i is the frequency of the ith mode). The following theorem gives the necessary and sufficient conditions of controllability of the system defined by equations (4) and (6), with respect to the torque vector T (or force vector f).

Theorem 1.- The system given by equations (4) and (6) is controllable with respect to $T(f)$ iff (if and only if): (i) the rigid-body system (eq. (4)) is controllable with respect to T, and (ii) for the flexible part, for $i=1,2,\ldots,n_q$, if (a) λ_i is a simple eigenvalue, $\Phi_t(j,i) \neq 0$ for some $j \in [1,n_t]$

(b) if λ_i has multiplicity μ_i, then rank of the $n_t \times \mu_i$ block of Φ_t ($n_f \times \mu_i$ block) corresponding to λ_i is μ_i. Similar results hold for force input f.

Outline of proof.- It has been proved in reference 9 that the system given by equation (6) is completely controllable if conditions (iia) and (iib) hold. Considering the composite system given by equations (4) and (6), results of reference 10 can be applied in a straightforward manner to complete the proof.

Equation (6) does not include the damping term, which, although small, will always be present in practical LSS. When damping is represented, equation (6) becomes:

$$\ddot{q} + D\dot{q} + \Lambda q = \Phi_f^T f + \Phi_t^T T \tag{7}$$

where $D = D^T \geq 0$ is the $n_q \times n_q$ damping matrix. If the system is controllable for $D = 0$, it will be controllable for $D \geq 0$, for sufficiently small D (because of the continuity property). However, stabilizability of the system is more important, especially while designing LQG regulators. The following theorem gives sufficient condition for stabilizability.

Theorem 2.- The system given by equations (4) and (6) is stabilizable for $D \neq 0$ if it is controllable for $D = 0$.

Outline of proof.- By applying the results of reference 10, it can be proved that the system is stabilizable if condition (i) of theorem 1 is satisfied, and if the system of equation (6) is stabilizable. If the system of equation (6) is controllable, then there exists a rate feedback gain such that the closed-loop system (with $D \neq 0$) is asymptotically stable (ref. 6). Thus the system of equation (6) is stabilizable for $D \neq 0$. This completes the proof.

Since observability is the dual concept of controllability, theorems 1 and 2 can be used to also investigate observability. The plate model selected for the LSS study has a number of modes with repeated natural frequencies (multiplicity = 2). Using theorem 1 it is evident that at least two actuators will be required for controllability (necessary condition). It is straightforward to check controllability (and observability) with respect to given actuator (sensor) locations by applying theorem 1.

Actuator and Sensor Models

The controller design approach proposed in this report uses several Annular Momentum Control Devices (AMCD's) for damping enhancement, and torque actuators or AMCD's for primary attitude control. An AMCD (fig. 2) consists of a rotating thin rim which is suspended in three or more non-contacting electromagnetic actuators and driven by a noncontacting electromagnetic spin motor (ref. 7). The bandwidth of AMCD sensors and actuators is very high--of the order of hundreds of Hertz--therefore, AMCD sensors and actuators can be assumed to be without phase lag. In the AMCD model, only x and y axis rim rotations and z-axis rim translation need be considered. The basic linearized AMCD equations of motion may be found in references 11 and 12. Since AMCD's are assumed to be relatively small (of the order of 2 m rim diameter), the rims can be assumed to be rigid. Torque actuators and attitude/rate sensors (used for primary controller) are assumed to be linear and to have infinite-bandwidths. This assumption is justified in case of sensors since sensor bandwidths are expected to be several decades higher than LSS closed-loop rigid-body bandwidth, and modal frequencies of interest. Effects of finite bandwidth and nonlinearities in torque actuators are not considered in this report in order to be able to obtain certain fundamental results.

A TWO-LEVEL CONTROLLER DESIGN APPROACH

The controller design approach proposed in this report consists of a primary and a secondary controller. The function of the secondary controller is to enhance damping in LSS structural modes without attempting to control rigid-body modes. The secondary controller should be robust--that is, it

should be stable regardless of parameter inaccuracies. A secondary controller consisting of several AMCD's is proposed in this report. The advantages of using AMCD's are: (i) precise knowledge of modal frequencies and mode shapes is not required, (ii) the closed-loop system is Lyapunov-stable (asymptotically stable under certain conditions) regardless of parameter inaccuracies and regardless of number of modes in the model, as will be shown later, (iii) associated weight penalty is small, and (iv) the secondary controller using AMCD's imparts gyroscopic stability to LSS. The last feature may be useful during initial phases of deployment, assembly or initial in-orbit parameter estimation, before the primary attitude controller is activated or even designed.

Secondary controller design using a single AMCD was investigated in references 13 and 14, with the latter reference containing more detailed stability results. The case with several AMCD's was investigated in reference 15. Although the sufficient conditions obtained in reference 15 for Lyapunov stability are easy to satisfy, those for asymptotic stability (AS) are difficult to satisfy in practice. Simpler sufficient conditions for AS are presented in this report.

SECONDARY CONTROLLER USING AMCD'S

Mathematical Model of LSS/AMCD's

It is assumed that ν (≥ 1) AMCD's are used on an LSS of mass m_s, inertia matrix I_s (two-dimensional), and n_q structural bending modes. The AMCD rims are assumed to be relatively small ($\approx$2 m) in diameter; therefore, they can be considered to be rigid. Only x and y axis rotations and z-axis translations are considered, which suffices to present the principles.

The location of nominal rim center position of the ith AMCD in the LSS coordinates is (x_k, y_i). m_{a_i}, r_i, I_{a_i}, ℓ_i (≥ 3) represent the mass, rim radius, transverse-axis inertia matrix, and number of actuator stations for the ith AMCD. C_{1i} represents $2 \times \ell_i$ moment-arm matrix of the AMCD actuator stations, and C_{2i} is a $1 \times \ell_i$ vector consisting of all unity entires. ε_i represents the Z axis displacement of the ith AMCD rim center from the corresponding point on the LSS. Let $\alpha_s = (\phi_s, \theta_s)$ denote the LSS attitude vector about the x and y axes, and $\alpha_{ai} = (\phi_{ai}, \theta_{ai})$ denote the rim attitude vector for the ith rim. The actuator stations are assumed to produce only axial (z-axis) forces. (Only radial rim centering is accomplished by radial actuator forces and is of no consequence in the present analysis.)

From the basic principles of dynamics the combined AMCD/LSS equations of motion can be written as:

$$A\ddot{x} + B\dot{x} + Cx = Yf \tag{9}$$

$$x = (\alpha_s^T, \alpha_{a_1}^T - \alpha_s^T, \ldots, \alpha_{a_\nu}^T - \alpha_s^T, \varepsilon_1, \ldots, \varepsilon_\nu, q^T)^T \tag{10}$$

where q denotes the n_q-vector of modal amplitudes of the LSS

$$f = (F_1^T, F_2^T, \ldots, F_\nu^T)^T \tag{11}$$

$$F_i = (f_{i1}, f_{i2}, \ldots, f_{i\ell_i})^T \qquad i=1,2,\ldots,\nu \tag{12}$$

f_{ik} being the axial force at actuator station k of the ith AMCD.

A is a $(n_1 \times n_1)$ symmetric positive definite coefficient matrix (where $n_1 = n_q + 3\nu + 2$):

$$A = \begin{bmatrix} A_1 & 0 \\ (3\nu + 2) \times (3\nu + 2) & \\ 0 & I_{n_q \times n_q} \end{bmatrix}$$

$I_{n_q x n_q}$ denotes the $n_q x n_q$ identity matrix

$$A_1^{-1} = \left[\begin{array}{c|ccc|c} I_s^{-1} & -I_s^{-1} & \cdots & -I_s^{-1} & -I_s^{-1}\zeta_1 \cdots -I_s^{-1}\zeta_\nu \\ \hline -I_s^{-1} & I_s^{-1} + I_{a_1}^{-1} & \cdots & I_s^{-1} & I_s^{-1}\zeta_1 \cdots I_s^{-1}\zeta_\nu \\ -I_s^{-1} & I_s^{-1} & I_s^{-1} + I_{a_2}^{-1} \cdots & I_s^{-1} & I_s^{-1}\zeta_1 \quad I_s^{-1}\zeta_\nu \\ \vdots & \vdots & \vdots & \vdots & \vdots \quad \vdots \\ -I_s^{-1} & I_s^{-1} & \cdots & I_s^{-1} + I_{a_\nu}^{-1} & I_s^{-1}\zeta_1 \cdots I_s^{-1}\zeta_\nu \\ \hline -\zeta_1^T I_s^{-1} & \zeta_1^T I_s^{-1} & \cdots & \zeta_\nu^T I_s^{-1} & \\ \vdots & \vdots & & \vdots & \\ & & & & \zeta I_s^{-1}\zeta^T + M_a^{-1} + \{M_s^{-1}\} \\ \vdots & \vdots & & \vdots & \\ -\zeta_\nu^T I_s^{-1} & \zeta_1^T I_s^{-1} & \cdots & \zeta_\nu^T I_s^{-1} & \end{array}\right]$$

(13)

where $\zeta = [\zeta_1, \ldots, \zeta_\nu]^T$, $\zeta_i = (y_i, -x_i)$, $M_a = \text{diag.}\ (m_{a_1}, \ldots, m_{a_\nu})$ and

$$\left\{M_s^{-1}\right\}_{ij} = 1/m_s$$

$$B = \left[\begin{array}{c|ccc|cc} \sum_{i=1}^{\nu} W_i & W_1 & W_2 \cdots & W_\nu & 0 & 0 \\ \hline W_1 & W_1 & 0 & & & \\ \vdots & & W_2 \ddots & & 0 & 0 \\ W_\nu & 0 & & W_\nu & & \\ \hline 0 & & 0 & & 0 & 0 \\ \hline 0 & & 0 & & 0 & D \end{array}\right] \qquad (14)$$

where $D = D^T \geq 0$ denotes the $n_q \times n_q$ LSS damping matrix.

$$W_i = \begin{bmatrix} 0 & H_i \\ -H_i & 0 \end{bmatrix} \qquad (15)$$

H_i being the angular momentum of the ith rim about the Z axis.

$$C = \left[\begin{array}{c|c} 0_{(3\nu + 2) \times (3\nu + 2)} & 0 \\ \hline 0 & \Lambda_{n_q \times n_q} \end{array}\right] \tag{16}$$

Where $\Lambda = \Lambda^T > 0$ is the LSS modal frequency matrix (usually diagonal, with squared modal frequencies as its entries).

$$\gamma = \left[\begin{array}{cccc} 0_{2\times 2} & 0 & \cdot\ \cdot & 0 \\ \hline C_{11} & 0 & \cdot\ \cdot & 0 \\ 0 & C_{12} & \cdot\ \cdot & 0 \\ \cdot & & & \\ \cdot & & & \\ 0 & 0 & & C_{1\nu} \\ \hline C_{21} & 0 & \cdot\ \cdot & 0 \\ 0 & C_{22} & \cdot\ \cdot & 0 \\ \cdot & & & \\ \cdot & & & \\ 0 & \cdot & \cdot\ \cdot & C_{2\nu} \\ \hline -\Phi_1^T & -\Phi_2^T & & -\Phi_\nu^T \end{array}\right]_{n_1 \times \ell} \triangleq \left[\begin{array}{c} 0_{2\times \ell} \\ \hline \eta_{n_2 \times \ell} \end{array}\right] \tag{17}$$

Φ_i $(i=1,2,\ldots, \nu)$ represents the $\ell_i \times n_q$ mode shape matrix for actuator locations of the ith AMCD, $\ell = \sum_{i=1}^{\nu} \ell_i$, and $n_2 = n_q + 3\nu (\stackrel{\Delta}{=}$ in eq. (17) denotes equality by definition).

Let δ_{ik} be the axial centering error at actuator station k of the ith AMCD. The $\ell \times 1$ centering error vector δ is given by

$$\delta = (\delta_{11},\ldots, \delta_{1\ell_1},\ldots, \delta_{\nu 1},\ldots, \delta_{\nu\ell_\nu})^T$$

$$= -\gamma^T x \tag{18}$$

Closed-Loop Stability

Consider a control law of the type

$$f = K_p\delta + K_r\dot{\delta} \tag{19}$$

Where K_p and K_r are real symmetric positive definite $\ell \times \ell$ proportional and rate gain matrices.

It was proved in reference 15 that the closed-loop system given by equations (9) and (19) has at least two zero eigenvalues for all K_p and K_r. The zero eigenvalues correspond to α_s which represents LSS rigid-body attitude. Defining:

$$p = (\alpha_{a_1}^T - \alpha_s^T, \ldots, \alpha_{a_\nu}^T - \alpha_s^T, \varepsilon_1, \ldots, \varepsilon_\nu, q^T)^T \tag{20}$$

$$\tilde{x} = (p^T, \dot{x}^T)^T = (p^T, \dot{\alpha}_s^T, \dot{p}^T)^T \tag{21}$$

Equation (9) (excluding α_s) can be expressed as:

$$\dot{\tilde{x}} = \tilde{A}\,\tilde{x} + \tilde{B}\,f \tag{22}$$

where

$$\tilde{A} = \left[\begin{array}{c|c|c} 0_{n_2 \times n_2} & 0_{n_2 \times 2} & I_{n_2 \times n_2} \\ \hline -A^{-1}\left(\begin{array}{c} 0_{(3\nu+2)\times n_2} \\ \hline 0_{n_q \times 3\nu} \end{array} \;\middle|\; \Lambda\right) & & -A^{-1}\,B \end{array}\right] \tag{23}$$

($I_{m\times m}$ denotes the $m\times m$ identity matrix)

$$\tilde{B} = \begin{bmatrix} 0_{n_2\times \ell} \\ \hline A^{-1}\begin{pmatrix} 0_{2\times \ell} \\ \eta_{n_2\times \ell} \end{pmatrix} \end{bmatrix} \tag{24}$$

It was proved in reference 15 that the closed-loop system is Lyapunov-stable if $K_p > 0$, $K_r \geq 0$, and is asymptotically stable if:

(i) $K_p > 0$, $K_r > 0$, (ii) $\sum_1^\nu H_i \neq 0$, (iii) $\ell \geq n_q + 3\nu$, (iv) rank $(\gamma) = n_q + 3\nu$. However, conditions (iii) and (iv) are difficult to satisfy in practice. In order to obtain the least restrictive (necessary and sufficient) conditions, it is first proved that the control law of Equation (19) is optimal with respect to a certain linear quadratic performance index.

Define the matrices

$$Q = \begin{bmatrix} \eta K_p R K_p \eta^T & 0 \\ 0 & \rho\Delta + \rho^2 \gamma R^{-1} \gamma^T \end{bmatrix} \tag{25}$$

where $\Delta = 2$ diag. $(0_{(3\nu+2)}, D)$, and $\rho > 0$ (scalar). γ is given by (17).

$$R = \rho K_r^{-1}, \quad \text{and} \quad S = \begin{bmatrix} \eta K_p R \\ 0_{n_1 \times \ell} \end{bmatrix}$$

Theorem 3.- The optimal control law (provided that it exists) which minimizes the performance function

$$J = \int_0^\infty (\tilde{x}^T Q \tilde{x} + 2\tilde{x}^T S f + f^T R f)\, dt \tag{26}$$

is given by equation (19).

Proof.- The proof can be obtained by comparing equation (11) with the standard solution of the LQ regulator problem (eq. (26)).

It can be shown that the Riccati matrix is given by

$$P = \rho \begin{bmatrix} \eta K_p \eta^T + \begin{pmatrix} 0 & 0 \\ 0 & \Lambda \end{pmatrix} & 0 \\ 0 & A \end{bmatrix} \tag{27}$$

It has been proved in reference 15 that the matrix $[\eta K_p \eta^T + \text{diag}\,(0,\Lambda)] > 0$. Therefore, $P > 0$.

Stability results.- Well established stability properties of the closed-loop optimal LQ regulator can be used for investigating the asymptotic stability of the system. The AMCD/LSS system consists of the two subsystems represented by the following set of equations:

$$S_1: \quad \dot{x}_1 = \tilde{A}_1 x_1 + \tilde{B}_1 f \tag{28}$$

$$S_2: \quad \dot{x}_2 = \tilde{A}_2 x_2 + \tilde{B}_2 f \tag{29}$$

where

$$x_1 = (\alpha_{a_1}^T - \alpha_s^T, \ldots, \alpha_{a_\nu}^T - \alpha_s^T, \varepsilon_1, \ldots \varepsilon_\nu, \dot{\alpha}_s^T, \dot{\alpha}_{a_1}^T - \dot{\alpha}_s^T, \ldots, \dot{\alpha}_{a_\nu}^T - \dot{\alpha}_s^T, \dot{\varepsilon}_1, \ldots, \dot{\varepsilon}_\nu)^T \tag{30}$$

$$x_2 = (q^T, \dot{q}^T)^T \tag{31}$$

$$\tilde{A}_1 = \left[\begin{array}{c|cc} 0_{3\nu\times 3\nu} & 0_{3\nu\times 2} & I_{3\nu\times 3\nu} \\ \hline 0_{(3\nu+2)\times 3\nu} & & -A_1^{-1}B_1 \end{array}\right], \quad \tilde{B}_1 = \left[\begin{array}{c} 0 \\ \hline A_1^{-1}\begin{pmatrix} 0 \\ L \end{pmatrix} \end{array}\right]$$

where A_1 and B_1 represent the top $3\nu \times 3\nu$ submatrices of A and B, and L is the $3\nu \times \ell$ matrix consisting of the top 3ν rows of η.

$$\tilde{A}_2 = \begin{bmatrix} 0 & I_{n_q \times n_q} \\ -\Lambda & -D \end{bmatrix}, \quad \tilde{B}_2 = \begin{bmatrix} 0 \\ -\Phi^T \end{bmatrix}$$

Since $\ell_i \geq 3$ for all i and actuators are at distinct locations, rank (L) = 3ν. Equation (29) can be transformed into the controllable canonical form:

$$\begin{bmatrix} \dot{r}_1 \\ \dot{r}_2 \end{bmatrix} = \begin{bmatrix} \alpha_{11} & \alpha_{12} \\ 0 & \alpha_{22} \end{bmatrix} + \begin{bmatrix} \psi \\ 0 \end{bmatrix} f$$

where the dimension of r_1 is n_c ($\leq 2\, n_q$) and that of r_2 is $2n_q - n_c$. α_{11}, α_{12}, α_{22} and ψ are appropriately dimensioned matrices.

Theorem 4.- The optimal control law for the problem in Theorem 1 exists, and the system of equation (22) with the control law of equation (19) is asymptotically stable, iff (if and only if) all the following conditions are satisfied.

(a) the pair $(\tilde{A}_2, \tilde{B}_2)$ is stabilizable.

(b) $\sum_{i=1}^{\nu} W_i \neq 0$

(c)

$$\text{rank} \begin{bmatrix} B_1 \pm 2j\Omega_i A_1 & 0 & \begin{pmatrix} 0 \\ L \end{pmatrix} \\ 0 & \alpha_{11} \pm 2j\Omega_i I_{n_c \times n_c} & \psi \end{bmatrix} = n_c + 3\nu + 2$$

for all i $(i=1,2,\ldots, \nu)$ for which $\Omega_i \neq 0$, where Ω_i = spin velocity of the ith AMCD rim.

Proof.- From linear-quadratic optimal regulator theory, it is well known that the control law of equation (19) makes the closed-loop system asymptotically stable if and only if (1) $(\hat{A}, \tilde{B})$ is stabilizable, where $\hat{A} = \tilde{A} - \tilde{B} R^{-1} S^T$, and (2) $(\hat{A}, \hat{C})$ is detectable, where $Q = \hat{C} \hat{C}^T$ (ref. 16). Also, P is positive definite if and only if $(\hat{A}, \hat{C})$ is observable; thus statement (2) above is true since $P > 0$. Stabilizability of $(\hat{A}, \tilde{B})$ is equivalent to that of $(\tilde{A}, \tilde{B})$ (ref. 17), which is equivalent to (1) stability of α_{22} and (2) controllability of the composite system consisting of equation (28) and the equation:

$$\dot{r}_1 = \alpha_{11}\, r_1 + \psi f$$

This composite system is controllable if and only if (α_{11}, ψ) is controllable and rank (c) = $n_c + 6\nu + 2$ where

$$c = \begin{bmatrix} \tilde{A}_1 - \lambda_i\, I_{(6\nu+2)\times(6\nu+2)} & 0 & \tilde{B}_1 \\ 0 & \alpha_{11} - \lambda_i I_{n_c \times n_c} & \psi \end{bmatrix} \qquad (32)$$

and where λ_i is the ith eigenvalue of $\tilde{A}_1$ (ref. 10). Assuming the AMCD rims to be thin it can be verified that the eigenvalues of $\tilde{A}_1$ are: 0, $\pm 2j\Omega_i$, where Ω_i is the spin velocity of the ith rim. The proof can be completed by using elementary matrix operations.

These necessary and sufficient conditions are not straightforward to apply. The following corollary gives sufficient conditions for asymptotic stability which are more easily applicable.

Corollary 1.- The system of equation (22) with the control law of equation (19) is asymptotically stable if all the three conditions given below are satisfied: (a) the LSS structural model, i.e., the pair $(\tilde{A}_2, \tilde{B}_2)$ is stabilizable, (b) $\sum_{i=1}^{\nu} W_i \neq 0$, and (c) the LSS does not have an undamped structural mode with frequency $2\Omega_i$ $(i=1,2,\ldots, \nu)$.

Proof.- Since $\pm j2\Omega_i$ is not an eigenvalue of α_{11}, it remains to be proved only that (Theorem 2)

$$\text{rank} \left[B_1 \pm j2\Omega_i A_1 \;\vdots\; \begin{pmatrix} 0 \\ L \end{pmatrix} \right] = 3\nu + 2 \tag{33}$$

for $\Omega_i \neq 0$.

Or equivalently that

$$\text{rank} \left[A_1^{-1} B_1 \pm j2\Omega_i \;\vdots\; A_1^{-1} \quad \begin{pmatrix} 0 \\ L \end{pmatrix} \right] = 3\nu + 2 \tag{34}$$

By applying elementary row operations and using the fact that rank $(C_{1i}) = 2$, $(i=1,2,\ldots, \nu)$, the rank of the matrix in equation (34) can be shown to be $3\nu + 2$ for $\Omega_i \neq 0$. Thus from Theorem 4, the system is asymptotically stable.

The following corollary generalizes the sufficient conditions which were derived in reference 15. It should be noted that they are too restrictive since they require a large number of actuators, and are given here only for completeness.

Corollary 2.- The system in equation (22) with the control law of equation (19) is asymptotically stable if all four conditions given below are satisfied:

(a) The LSS structural model, i.e., the pair $(\tilde{A}_2, \tilde{B}_2)$ is stabilizable; (b) $\sum_{1}^{\nu} W_i \neq 0$; (c) $\ell \geq n_c + 3\nu$, and (d) rank $(\gamma) = n_c + 3\nu$.

Proof.- Since rank $(\gamma) = n_c + 3\nu$, rank $\begin{bmatrix} L \\ \psi \end{bmatrix} = n_c + 3\nu$. Condition (c) of Theorem 4 is satisfied if for $\lambda = \pm j2\Omega_i$,

$$\text{rank} \left[\begin{array}{c|c} B_1 \pm \lambda A_1 & \begin{pmatrix} 0 \\ L \end{pmatrix} \\ \hline 0 & \psi \end{array}\right] = n_c + 3\nu + 2$$

Since rank $\begin{bmatrix} L \\ \psi \end{bmatrix} = 3\nu$, condition (c) of Theorem 4 is satisfied if the two top rows of $B_1 - \lambda A_1$ are independent for $\lambda = \pm 2j\Omega_i$. It can be verified that this is indeed the case.

The sufficient conditions in corollary 1 are less restrictive than those in corollary 2 because the former do not require a large number of actuators.

It should be noted that, in addition to strutural damping enhancement, the secondary controller also imparts gyroscopic stability to the LSS (rigid-body attitude). This feature should be useful during assembly and during initial operations (such as parameter identification) in a newly deployed or assembled LSS, before the primary controller is activated, or even designed.

PRIMARY ATTITUDE CONTROL SYSTEM

The secondary control system increases modal damping and thus controls the shape of LSS. It also aids in primary controller design by reducing the effect of "spillovers." In this report, primary attitude controller design is considered using torque actuators and AMCD's. A primary attitude control system using torque actuators is considered first.

Primary Controller Using Torque Actuators

Assuming that the primary attitude control is accomplished using σ (≥ 1) two-axis torque actuators distributed on the LSS, the LSS equations of motion (without secondary controller) are given by:

$$A_s \ddot{x}_s + B_s \dot{x}_s + C_s x_s = \sum_{i=1}^{\sigma} \gamma_{ti} T_i \tag{35}$$

where $x_s = (\alpha_s^T, q^T)^T$, $A_s = \text{diag.}\,(I_s, I_{n_q \times n_q})$, $B_s = \text{diag.}\,(0, D)$, $C_s = \text{diag.}\,(0, \Lambda)$.

$$\gamma_{ti} = \begin{bmatrix} I_{2\times 2} \\ \Phi_{mi}^T \end{bmatrix}, \quad T_i = \begin{bmatrix} T_{xi} \\ T_{yi} \end{bmatrix} \tag{36}$$

Φ_{mi} being the $2 \times n_q$ "torque mode-shape matrix" corresponding to location of actuator i. T_{xi} and T_{yi} are the x and y axis torques.

Colocated actuators and sensors.- Assuming that σ, two-axis attitude and rate sensors are also located at the same points as the torque actuators, the measured attitude vector α_{mi} and the measured attitude rate vector α_{mri} at location i (ignoring noise) are given by:

$$\alpha_{mi} = \gamma_{ti}^T x_s \tag{37}$$

$$\alpha_{mri} = \gamma_{ti}^T \dot{x}_s \tag{38}$$

Denoting $\Gamma = [\gamma_{t1}, \ldots, \gamma_{t\sigma}]$, $T = (T_1^T, \ldots T_\sigma^T)^T$, $\alpha_m = [\alpha_{m_1}^T, \ldots, \alpha_{m\sigma}^T]^T$ $\alpha_{mr} = [\alpha_{mr1}^T, \ldots, \alpha_{mr\sigma}^T]^T$ equations (35), (37), and (38) can be written as:

$$A_s \ddot{x}_s + B_s \dot{x}_s + C_s x_s = \Gamma T \tag{39}$$

$$\alpha_m = \Gamma^T x_s \tag{40}$$

$$\alpha_{mr} = \Gamma^T \dot{x}_s \tag{41}$$

Choosing the control law

$$T = -(G_p \alpha_m + G_r \alpha_{mr}) \tag{42}$$

where G_p and G_r are $2\sigma \times 2\sigma$ positive definite symmetric matrices. For example, a simple control law for controlling the rigid-body attitude would be:

$$T_i = \frac{1}{\sigma} I_s \left[\begin{pmatrix} 2\rho_s\omega_{sx} & 0 \\ 0 & 2\rho_y\omega_{sy} \end{pmatrix} \alpha_{mri} + \begin{pmatrix} \omega_{sx}^2 & 0 \\ 0 & \omega_{sy}^2 \end{pmatrix} \alpha_{mi} \right] \tag{43}$$

for $i=1,2,\ldots, \sigma$, where ρ_{sk} and ω_{sk} $(k = x,y)$ denote the desired rigid-body damping ratio and natural frequency. In this case G_p and G_r will be block-diagonal matrices.

The closed-loop equations become:

$$A_s\ddot{x}_s + (B_s + \Gamma G_r \Gamma^T)\dot{x}_s + (C_s + \Gamma G_p \Gamma^T)x_s = 0 \tag{44}$$

Finally, the AMCD loops may be closed using equations (18) and (19).

Theorem 5.- The system of equation (44) is stable in the sense of Lyapunov if $G_p > 0$, $G_r \geq 0$.

Proof.- Considering a Lyapunov function:

$$V(x_s, \dot{x}_s) = x_s^T \bar{C}_s x_s + \dot{x}_s^T A_s \dot{x}_s \tag{45}$$

where $\bar{C}_s = C_s + \Gamma G_p \Gamma^T$. It can be shown that $\bar{C}_s > 0$, and that:

$$\dot{V} = -\dot{x}_s^T \bar{B}_s \dot{x}_s \leq 0 \tag{46}$$

(since $\bar{B}_s = B_s + \Gamma G_r \Gamma^T \geq 0$).

Thus, the primary control law using colocated torque actuators and attitude and rate sensors gives a stable closed-loop system. The controller is robust because it is stable regardless of parameter inaccuracies. In addition to controlling rigid-body modes, the "colocated" primary controller also increases damping in some of the structural modes, depending on the locations of torque actuators. The secondary controller consisting of AMCD's can be added in order to enhance modal damping and improve the overall performance. When the secondary controller is included, it can be shown that the overall closed-loop system is Lyapunov stable if $G_p > 0$, $G_r \geq 0$, $K_p > 0$ and $K_r \geq 0$.

Noncolocated actuators and sensors.- Stability of the closed-loop system is no longer guaranteed when actuators and sensors of the primary controller are not colocated. This is because of control and observation "spillovers." In reference 3, the following controller design approaches based on LQG control theory were investigated:

1. Truncation: In this method, the residual (uncontrolled) structural modes are merely ignored in the design process.

2. Modified Truncation (or Model Error Sensitivity Suppression, Reference 18): The effect of control input on selected residual modes is included in the performance function in a quasi-static sense.

3. Use of Higher-Order Estimator: In this method, the state estimator estimates more modal amplitudes and rates than are fed back.

4. Selective Modal Suppression: Observation spillover for selected residual modes is reduced or eliminated by using such devices as phase-lock-loops.

5. Polynomial Estimators: Observation spillover is explicitly estimated by representing it as a polynomial in time.

These methods typically result in a controller which consists of a linear regulator and a Kalman-Bucy filter for state estimation. It was reported in reference 3 that, when a sufficient number of sensor outputs are available, better results are obtained using direct sensor feedback (DSF) than using state estimators. Of the methods considered in reference 3, method 5 was reported to be unsatisfactory. Preliminary numerical results obtained by applying methods 1 to 4 to the plate mode (discussed previously) indicated

that the modified truncation {or Model Error Sensitivity Suppression (MESS)} method was the most promising method. Therefore, only the truncation method (being the most straightforward) and MESS method (being the most promising) are discussed in this report. As stated earlier, DSF was reported to result in better performance; therefore DSF is used in this report instead of state estimators. As a simple but important special case, it is assumed in the following analysis that the primary controller controls only rigid-body attitude, without attempting to actively control any structural modes. This assumption is justified to some extent because structural modes will be controlled by the secondary controller. In order to simplify implementation, the primary control law is constrained to require feedback of only measured attitude and rate (measured attitude and rate includes contributions of rigid-body and structural modes). It should be noted that this special case is included only for the purpose of demonstration and that primary controller design using truncation or MESS methods is not restricted to active control of rigid-body modes only.

MESS method - a special case: Assuming that the primary controller is to be designed to control only rigid-body modes α_s $[=(\phi_s,\theta_s)]$, and for the case with a single 2-axis torque actuator, consider the control law given by

$$T = \begin{bmatrix} T_x \\ T_y \end{bmatrix} = I_s \left[\begin{pmatrix} \omega_x^2 & 0 \\ 0 & \omega_y^2 \end{pmatrix} \alpha_{sm} + \begin{pmatrix} \rho_x^2 R_x^{-1} & 0 \\ 0 & \rho_y^2 R_y^{-1} \end{pmatrix} \omega_{sm} \right] \qquad (47)$$

where ω_i, ρ_i $(i = x,y)$ denote the desired rigid-body bandwidth and damping ratio, and α_{sm}, ω_{sm} denote the measured attitude and rate vectors; $R_i = 1/2\omega_i$. If control spillover were absent (i.e., if the actuators could force only rigid-body modes), this control law would minimize the performance function

$$J_o = \int_o^\infty \left\{ \alpha_s^T \begin{bmatrix} \omega_x^4 R_x & 0 \\ 0 & \omega_y^4 R_y \end{bmatrix} \alpha_s + \dot{\alpha}_s^T \begin{bmatrix} \rho_x^2 R_s^{-1} & 0 \\ 0 & \rho_y R_y^{-1} \end{bmatrix} \right.$$

$$\left. + 2\alpha_s^T \begin{bmatrix} R_x \omega_x^2 & 0 \\ 0 & R_y \omega_y^2 \end{bmatrix} T + T^T \begin{bmatrix} R_x & 0 \\ 0 & R_y \end{bmatrix} T \right\} dt \qquad (48)$$

This can be verified along the lines of reference 6. However, because of flexibility, the control input also forces structural modes. The model error sensitivity suppression method requires augmentation of a quadratic function of the forcing terms corresponding to a few selected structural modes, to the performance function in equation (48). If modes $k_1,\ldots k_p$ are selected for augmentation, denoting the mode shapes (for the kth mode) at the actuator location by ϕ_{xk} and ϕ_{yk}, the modified performance function becomes

$$J = J_o + \sum_{k=k_1}^{k_p} Q_k T^T \begin{bmatrix} \phi_{xk}^2 & \phi_{xk}\phi_{yk} \\ \phi_{xk}\phi_{yk} & \phi_{yk}^2 \end{bmatrix} T \qquad (49)$$

where Q_k is a positive weighting coefficient. The effect of addition of this term to the performance function is to modify the control weighting matrix. The optimal control law for this type of performance index requires feedback only of measured attitude and rate. A modified state estimator can be similarly designed for generating estimates of rigid-body attitude and rate.

Primary Attitude Control Using AMCD's

Instead of torque actuators, AMCD's can be used for primary attitude control. In particular, the AMCD's used for implementing a secondary controller can be simultaneously used for the actuation of the primary attitude controller. Primary attitude control is accomplished by torquing against AMCD momenta. In this dual control mode, however, the relative rotation angles between the LSS and the AMCD's (i.e., $\alpha_{a_i} - \alpha_s$, $i=1,2,..,\nu$) cannot be controlled simultaneously with LSS rigid-body attitude α_s (controllability of AMCD/rigid-body modes is discussed in reference 12). This entails that the control law of equation (19) for the secondary controller should be redesigned to exclude feedback of $(\alpha_{a_i} - \alpha_s)$. However, the rates $(\dot{\alpha}_{a_i} - \dot{\alpha}_s)$ must be zero in steady-state and must be fed back. That is, the position feedback gain must be redesigned to control only ε_i, the motion of the AMCD

rim centers relative to the LSS, and AMCD rim transverse rotation angles are allowed to be nonzero in steady-state. Provided that relative angles, $\alpha_{a_i} - \alpha_s$ are sufficiently small (so that the actuator gap limits are not exceeded), the AMCD's can be used in this dual control mode.

Columns of the $2 \times \ell_i$ matrix C_{1i} are given by $(y_{ij}, -x_{ij})$, $j=1,2,\ldots, \ell_i$. Since actuators of each AMCD are located along a circle, columns 1 and 2 are linearly independent, and columns 3 through ℓ_i can be expressed as linear combinations of the first two columns. That is, C_{1i} can be expressed as:

$$C_{1i} = c_i[I_2 \,\vdots\, \Gamma_i] \tag{50}$$

where c_i is the 2×2 matrix formed by the first two columns of C_{1i}, I_2 is the 2×2 identity matrix, and Γ_i is a $2 \times (\ell_i - 2)$ matrix. If K_p is designed as follows:

$$K_p = \text{diag}\left[\begin{pmatrix}\Gamma_1\\ -I\end{pmatrix}, \ldots, \begin{pmatrix}\Gamma_\nu\\ -I\end{pmatrix}\right] \tilde{K}_p \, \text{diag}\left[\begin{pmatrix}\Gamma_1\\ -I\end{pmatrix}, \ldots, \begin{pmatrix}\Gamma_\nu\\ -I\end{pmatrix}\right]^T \tag{51}$$

where $\tilde{K}_p$ is a $(\ell-2\nu)x(\ell-2\nu)$ positive definite matrix, and diag. ( ) denotes a block-diagonal matrix, it can be verified that the resulting coefficient matrix multiplying $(\alpha_{a_1}^T - \alpha_s^T, \ldots, \alpha_{a_\nu}^T - \alpha_s^T)^T$ in equation 19 (after substituting for δ from equation 18) is zero. Defining

$$h = (\varepsilon^T, q^T)^T \tag{52}$$

the resulting closed-loop system is the form:

$$\begin{bmatrix} \dot{h} \\ \dot{x} \end{bmatrix} = \left[\begin{array}{c|c|c} 0 & 0 & I \\ \hline \alpha_1 & \alpha_2 & \end{array}\right] \begin{bmatrix} h \\ x \end{bmatrix} \tag{53}$$

where α_1, α_2 are appropriately dimensioned matrices.

Theorem 6.- The system defined by equation (53) is stable in the sense of Lyapunov if $\tilde{K}_p > 0$ and $K_r \geq 0$.

Outline of proof.- The proof is similar to that of Theorem 2 (part a) in reference 15, except that it is additionally necessary to prove that $C_2 K_p C_2^T > 0$ (positive definite) for the specially structured K_p of equation (51). This can be proved by establishing that $z^T C_2 K_p C_2^T z$ can be zero for some $z \neq 0$ if and only if

$$[\Gamma_i^T, -I]\, C_{2i}^T = 0 \quad (i=1,2,\ldots, \nu) \tag{54}$$

Using the fact that actuators for each AMCD are located along a circle, it can be proved that equation (54) cannot hold. Therefore,

$$C_2 K_p C_2^T > 0$$

This type of secondary controller essentially provides rate feedback for modal damping enhancement. The only function of position gain is to keep the AMCD rim centers at their nominal positions. Additional force commands can now be superimposed on the electromagnetic actuators in order to produce the desired primary control torque for controlling α_s. Since AMCD's are small compared to the LSS, the effect of control moments generated in this manner would approximate point-torque actuators. If an attitude sensor and a rate sensor are located on the LSS at the nominal position of the center of each AMCD, this configuration would approximate colocated torque actuators and attitude/rate sensors, and should therefore have the associated Lyapunov-stability property. In this configuration, the AMCD's must have sufficiently large momenta in order to exert the magnitude of torque required to achieve the desired rigid-body bandwidth (without exceeding the electromagnetic actuator gap limits). Separate AMCD's may also be used for primary control actuation. The position gains for the rim suspension control system should be structured as discussed above to retain the closed-loop stability properties of the structural modes. For orbital applications it will be necessary to gimbal the AMCD's for primary controller actuation.

NUMERICAL RESULTS

For the purpose of demonstration of the primary and secondary controller design methods, the 44-mode finite element model of a 30.48 m × 30.48 m × 2.54 mm (100 ft × 100 ft × 0.1 in.), completely free, aluminum plate (discussed earlier) was used. The inherent damping ratios of all the structural modes were assumed to be zero. The AMCD's were chosen to have rims having 1.79 m

diameter and 34 kg mass, suspended in four equally spaced electromagnetic actuators and spinning at 5000 RPM. Secondary controller design was considered first.

Three AMCD's, centered at coordinates (4.44 m, -8.26 m), (-12.06 m, -0.635 m) and (14.6 m, -14.6 m) were used for the secondary controller (in the coordinate system with axes parallel to the plate edges and origin at the plate center). Gain matrices K_p and K_r were assumed to be diagonal, with entries k_{p_i}, k_{r_i} corresponding to the ith AMCD. Keeping the position gains constant at k_{p1} = 146 N/m, k_{p2} = 14.6 N/m, k_{p3} = 14.6 N/m, rate gains (k_{ri}) were increased for the three AMCD's, starting with zero rate gains. With $k_{r2} = k_{r3} = 0$, the gain k_{r1} was first increased starting from zero. Keeping k_{r1} constant at its nominal value of 5636 N-sec/m, and with $k_{r3} = 0$, k_{r2} was next increased from zero. Finally, with k_{r1} and k_{r2} fixed at their nominal values (k_{r1} as above and k_{r2} = 2050 N-sec/m), k_{r3} was increased from 0. As shown in the root loci of figure 3, damping ratios of the structural modes increase, the lowest damping ratio being 0.07 for nominal gains (i.e., position gains, k_{r1}, k_{r2} as above, and k_{r3} = 7174 N-sec/m). The root loci turn back towards the imaginary axis for higher rate gains. Although only the first seven modes are shown in figure 3, all modes exhibit similar behavior. Addition of each AMCD generally improves the closed loop damping ratios. Damping enhancement in different modes depends on the values of the mode shapes at the AMCD actuator locations.

Primary controller design using two-axis torque actuators and attitude/rate sensors was next considered. As discussed in the previous section, the primary controller was to be designed to control only rigid-body attitude, without attempting to actively control any structural modes.

Secondary controller gains (when used) were set at their nominal values given above. Numerical results were obtained using either a single torque actuator (2-axis) located at the center of the plate, or three torque actuators placed at the locations of AMCD centers given previously. Both colocated and noncolocated actuators/sensors cases were considered. For the noncolocated case, a single torque actuator located at the plate center was used, and the attitude and rate sensors were located at (15.24 m, 0 m). The "evaluation" or "truth model" for the noncolocated case was assumed to consist of rigid-body modes and the first seven structural modes. Numerical results were obtained for the following cases.

1. single primary actuator with noncolocated sensors - truncation method;
2. single primary actuator with noncolocated sensors - MESS method;
3. single primary actuator with colocated sensors; and
4. three distributed primary actuators with colocated sensors.

Numerical results for cases 1 through 4 were first obtained without the secondary controller, and then with the secondary controller (K_p and K_r being at their nominal values). The objective was to vary the primary controller position and rate feedback gains (or weighting coefficients Q_k in the case of MESS method) in order to get the highest rigid-body closed-loop bandwidth ω_{rb} with the restriction that the rigid-body damping ratio (ρ_{rb}) does not fall below 0.5 . Closed-loop damping ratios of the structural modes must also be reasonably high in order to obtain satisfactory shape/vibration control. Figure 4 shows a bar graph of ω_{max}, the maximum rigid-body bandwidth achieved such that $\rho_{rb} \geq 0.5$, and of ρ_{smin}, which represents the lowest closed-loop damping ratio for structural modes. Since the purpose of these computations was to gain some insight into performance of the methods discussed, formal numerical optimization routines were not used for obtaining ω_{max}; rather, it was accomplished by varying the parameters mentioned above and observing the trends. When the secondary controller was not used, computations revealed that it was

not possible to obtain a stable design for the noncolocated case with either truncation or MESS methods, as indicated by zero value of ω_{max} in figure 4. With the secondary controller included, however, stable designs were obtained for the noncolocated case, with the MESS method causing slight improvement over the truncation method. For the colocated cases, although closed-loop stability is guaranteed, it is possible to have zero closed-loop damping for some structural modes (with no secondary controller), as indicated by the results for case 3. In addition, because of interaction of structural modes, the maximum achievable rigid-body closed-loop bandwidth is also limited with this type of control law, although all eigenvalues are guaranteed to be in the closed left-half of the complex plane. The highest ω_{max} (about 0.05 rad/sec) was obtained using three distributed torque actuators with colocated sensors, when the secondary controller was included. It should be possible to increase it further by using additional AMCD's in the secondary controller. In all the cases considered, addition of secondary controller caused significant improvement. For investigating the use of the same AMCD's in primary and secondary controllers, preliminary numerical results were obtained for the case where attitude and rate sensors were located on the LSS at the AMCD center nominal locations. There was very little difference in the damping-enhancement characteristics in spite of using the specially structured K_p matrix. The overall closed-loop system was asymptotically stable even though the actuators/sensors in this case are only approximately colocated. However, it will be necessary to have larger total angular momentum in order to get a rigid-body closed-loop bandwidth of the order of 0.05 rad/sec.

PERFORMANCE EVALUATION

After primary and secondary controllers are designed to obtain satisfactory closed-loop dynamics (based on the known model parameters), the next step is evaluate the closed-loop performance in the presence of disturbances (such as gravity gradient, geomagnetic torques, solar pressure, etc.) and sensor/actuator noise. Gravity gradient and geomagnetic torque are slowly varying disturbances which need not be considered for investigating dynamic performance. (Depending on the LSS orbital configuration, they must be compensated for by using slowly varying input bias torques; however, they were not considered in this report since the scope of this investigation is limited to fine-pointing control over relatively short segments of time.) In the presence of disturbances and sensor/actuator noise,which can be described by zero-mean white noise, the overall closed-loop equations can be expressed as:

$$\dot{x}_c = A_c x_c + B_c v \tag{55}$$

where x_c is the n-dimensional state vector and v is a s-dimensional zero-mean white-noise with covariance intensity matrix V, which represents disturbances as well as sensor/actuator noise. A_c is the closed-loop system matrix, and B_c is the effective noise input matrix. Bandlimited white noise can also be represented by this formulation by incorporating the associated filter dynamics in A_c and B_c. The covariance of x_c evolves according to the equation:

$$\dot{\Sigma} = A_c \Sigma + \Sigma A_c^T + B_c V B_c^T \tag{56}$$

where $\Sigma = \mathcal{E}[x_c x_c^T]$.

In steady-state, $\dot{\Sigma} = 0$, and the resulting Lyapunov matrix equation can be solved for $\bar{\Sigma}$ (steady-state value of Σ) using one of the many available numerical methods. The method used in this report is that given in reference 19 since it was found to have good convergence properties. Closed-loop performance can be evaluated by examining elements of Σ. The x and y axis RMS pointing error at a particular point the LSS surface is given by:

$$\sigma_x^2 = \zeta_x^T \Sigma \zeta_x, \quad \sigma_y^2 = \zeta_y^T \Sigma \zeta_y \tag{57}$$

where the total attitude angles (ϕ about x-axis and θ about y-axis) are given by $\phi = \zeta_x^T x_c$ and $\theta = \zeta_y^T x_c$. The RMS (1 σ) and 3σ-errors at various points of interest on the LSS can be computed in this manner. It should be noted that it is necessary to have knowledge of the LSS parameters, disturbances and sensor/actuator noise in order to obtain reliable error estimates in this manner.

CONCLUDING REMARKS

A controller design approach for large space structures was presented, which consists of a primary attitude controller and a secondary or damping-enhancement controller. The primary controller uses either torque actuators

or Annular Momentum Control Devices (AMCD's) to control rigid body modes (and possibly some structural modes). The secondary controller uses several AMCD's and is shown to make the closed-loop system asymptotically stable under relatively simple conditions, regardless of parameter inaccuracies and number of structural modes in the model. The primary controller using torque actuators and colocated attitude and rate sensors is stable in the sense of Lyapunov (using positive definite feedback of measured attitude and nonnegative definite feedback of measured rate). A method for structuring the position feedback matrix was given, which permits the use of the same AMCD's for the actuation of primary and secondary controllers. Generic stability results, as well as numberical results obtained for a large, thin, completely free plate indicate that a control system consisting of a primary controller using several colocated actuators and sensors distributed on the LSS, and a secondary controller using several AMCD's, holds significant promise.

REFERENCES

1. Balas, M. J.: Feedback Control of Flexible Systems. IEEE Trans. Automatic Control, Vol. 23, No. 4, August 1978, pp. 673-679.
2. Joshi, S. M.; and Groom, N. J.: Stability Bounds for the Control of Large Space Structures. AIAA J. Guidance and Control, Vol. 2, No. 4, July-August, 1979, pp. 349-351.
3. Joshi, S. M.; and Groom, N. J.: Controller Design Approaches for Large Space Structures Using LOG Control Theory. Proceedings of second VPISU/AIAA Symposium on Dynamics and Control of Large Flexible Spacecraft, Blacksburg, Virginia, June 1979, pp. 35-50.
4. Balas, M. J.: Direct Velocity Feedback Control of Large Space Structures. AIAA J. Guidance and Control, Vol. 2, No. 3, May-June 1979.
5. Canavin, J. R.: Control Technology for Large Space Structures. AIAA Conference on Large Space Platforms, Los Angeles, California, September 1978. Paper No. 78-1691.
6. Aubrun, J. R.; Lyons, M.; Margulies, G.; Arbel, A.; and Gupta, N.: Stability Augmentation for Flexible Space Structures. 18th IEEE Conference on Decision and Control, Ft. Lauderdale, Florida, December 1979.
7. Anderson, W. W.; and Groom, N. J.: The Annular Momentum Control Device (AMCD) and Potential Applications. NASA TN D-7866, March 1975.
8. Joshi, S. M.; and Groom, N. J.: Finite Element Structural Model of a Large, Thin, Completely Free, Flat Plate. NASA TM-81887, September 1980.

9. Balas, M. J.: Active Control of Flexible Systems. Journal of Optimization Theory and Applications, Vol. 25, No. 3, July 1978, pp. 415-436.

10. Davison, E. J.; and Wang, S. H.: New Results on the Controllability and Observability of General Composite Systems. IEEE Trans. Automatic Control, Vol. AC-20, No. 1, February 1975, pp. 123-128.

11. Groom, N. J.: Fixed-Base and Two-Body Equations of Motion for an Annular Momentum Control Device (AMCD). NASA TM-78644, March 1978.

12. Nadkarni, A. A.; Groom, N. J.; and Joshi, S. M.: Optimal Fine-Pointing Control of a Large Space Telescope Using an AMCD. Proceedings of the 1977 IEEE SoutheastCon, Williamsburg, VA, April 4-6, 1977.

13. Joshi, S. M.; and Groom, N. J.: Modal Damping Enhancement in Large Space Structures Using AMCD's. AIAA J. Guidance and Control, VOL. 3 , No. 5 , September-October, 1980, pp. 477-479.

14. Joshi, S. M.; and Groom, N. J.: A Two-Level Controller Design Approach for Large Space Structures, 1980 Joint Automatic Conference, San Francisco, California, August 1980.

15. Joshi, S. M.: Damping Enhancement and Attitude Control of Large Space Structures. Proceedings of the 19th IEEE Conference on Decision and Control, Albuquerque, New Mexico, December 1980.

16. Kwakernaak, H.; and Sivan, R.: Linear Optimal Control Systems. Wiley-Interscience, 1972, pp. 237-238.

17. Wonham, W. M.: Linear Multivariable Control - A Geometric Approach. Springer-Verlag, 1974, p. 46.

18. Sesak, J. R.; Likins, P. W.; and Coradetti, T.: Flexible Spacecraft Control by Modal Error Sensitivity Suppression (MESS). J. Astronautical Sciences, Vol. 27, No. 2, April-June 1979, pp. 131-156.

19. Smith, P. G.: Numerical Solution of the Matrix Equation $AX + XA^T + B = 0$. IEEE Trans. Automat. Contr., Vol. AC-16, No. 3, June 1971, pp. 278-279.

TABLE I.- COMPUTED NATURAL FREQUENCIES OF PLATE STRUCTURAL MODEL

MODE	FREQ(RAD/SEC)	FREQ(HZ)
1	.54999E-01	.87534E-02
2	.80024E-01	.12736E-01
3	.99111E-01	.15774E-01
4	.14211E+00	.22618E-01
5	.14211E+00	.22618E-01
6	.24948E+00	.39707E-01
7	.24948E+00	.39707E-01
8	.26008E+00	.41392E-01
9	.28286E+00	.45018E-01
10	.31515E+00	.50157E-01
11	.43068E+00	.68545E-01
12	.43068E+00	.68545E-01
13	.47824E+00	.76114E-01
14	.50003E+00	.79583E-01
15	.53689E+00	.85449E-01
16	.53689E+00	.85449E-01
17	.62422E+00	.99347E-01
18	.65958E+00	.10497E+00
19	.68808E+00	.10951E+00
20	.80973E+00	.12887E+00
21	.80973E+00	.12887E+00
22	.83371E+00	.13269E+00
23	.87377E+00	.13906E+00
24	.87982E+00	.14003E+00
25	.87982E+00	.14003E+00
26	.99216E+00	.15791E+00
27	.99216E+00	.15791E+00
28	.11483E+01	.18275E+00
29	.11922E+01	.18974E+00
30	.11996E+01	.19093E+00
31	.12194E+01	.19407E+00
32	.12250E+01	.19497E+00
33	.12532E+01	.19946E+00
34	.12532E+01	.19946E+00
35	.13742E+01	.21872E+00
36	.14082E+01	.22412E+00
37	.14871E+01	.23668E+00
38	.14871E+01	.23668E+00
39	.16059E+01	.25558E+00
40	.16059E+01	.25558E+00
41	.16972E+01	.27012E+00
42	.16972E+01	.27012E+00
43	.17111E+01	.27233E+00
44	.17523E+01	.27889E+00

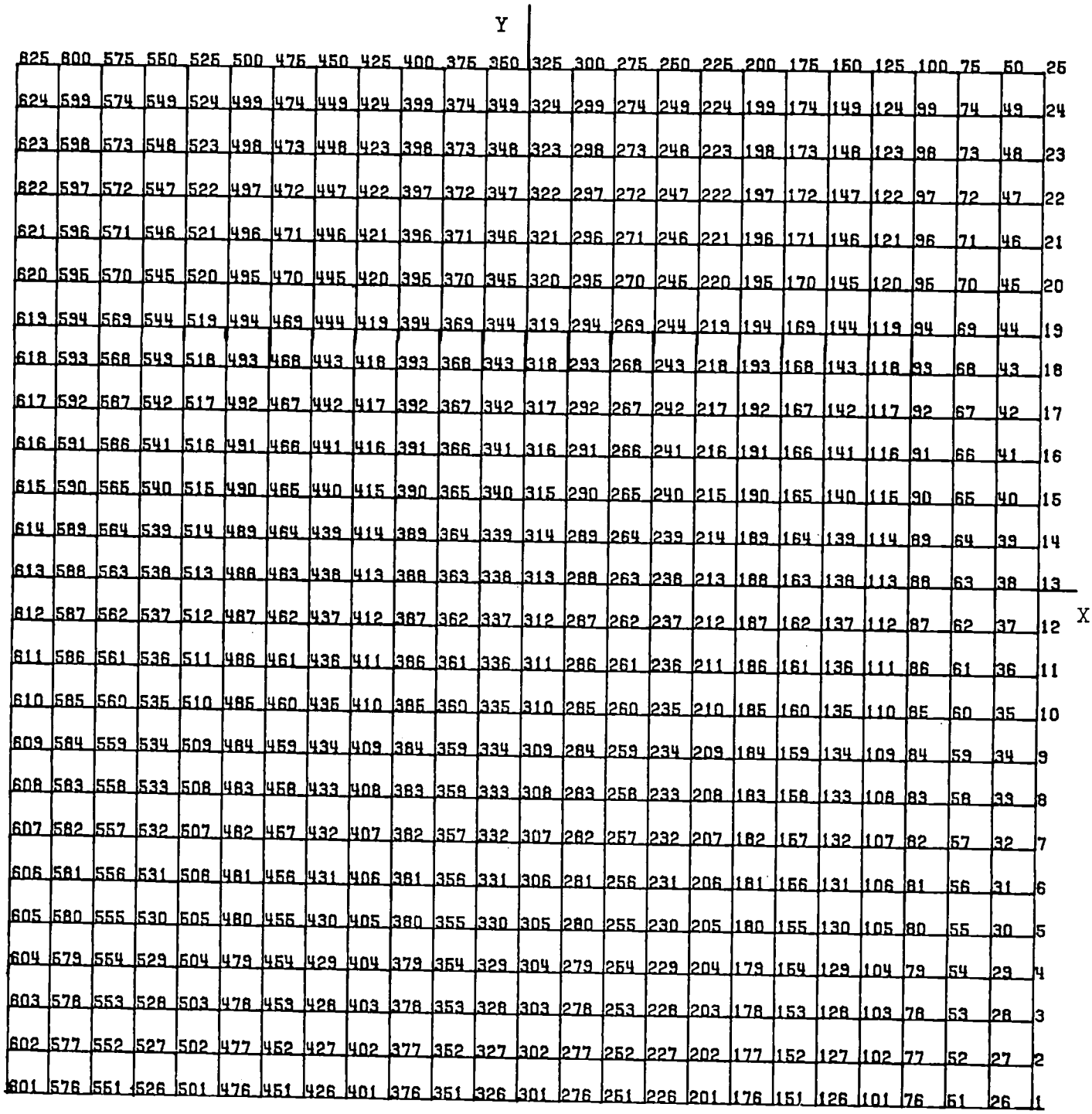

Figure 1.- Location of joints for plate structural model

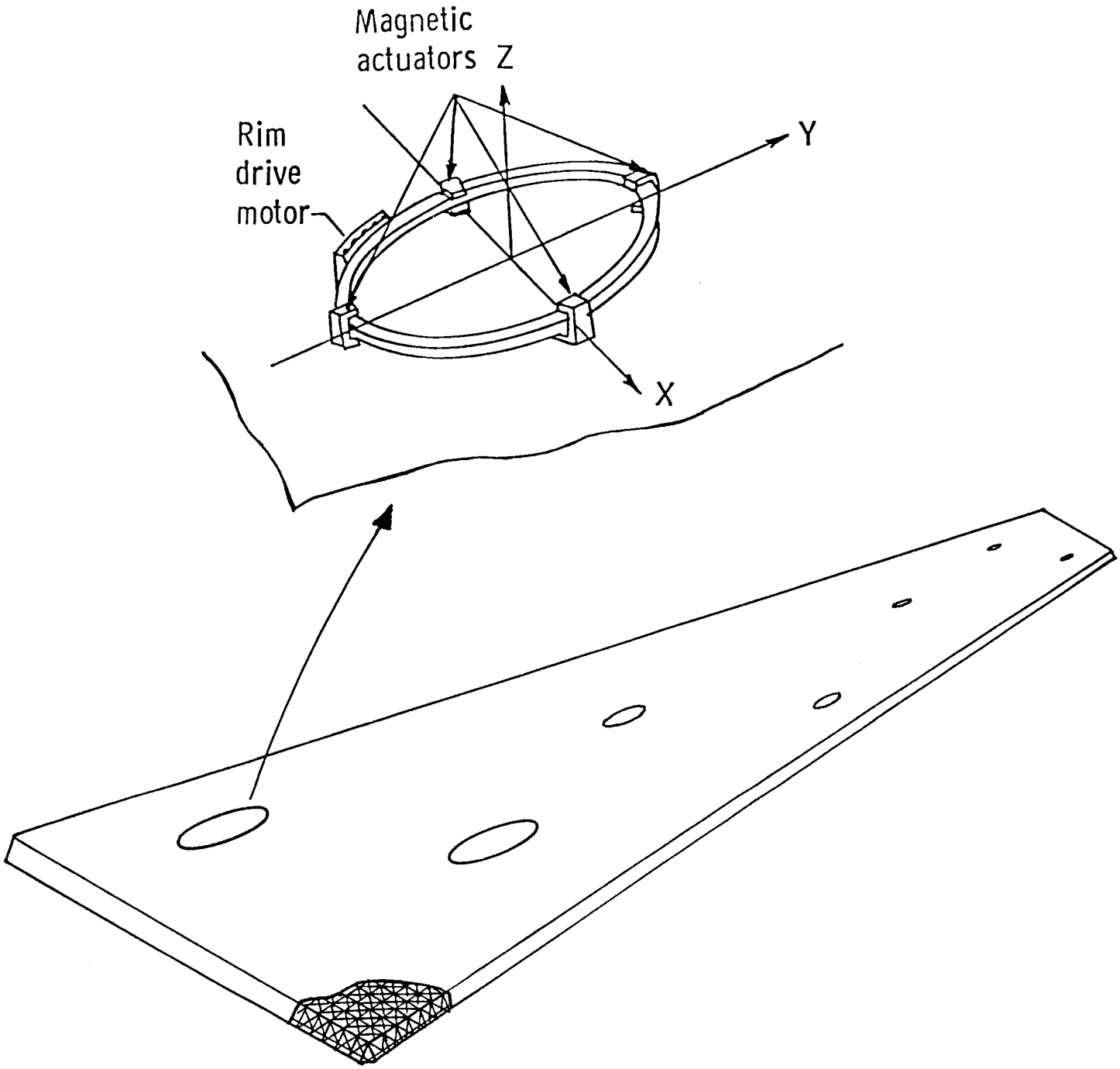

Figure 2.- AMCD/LSS configuration

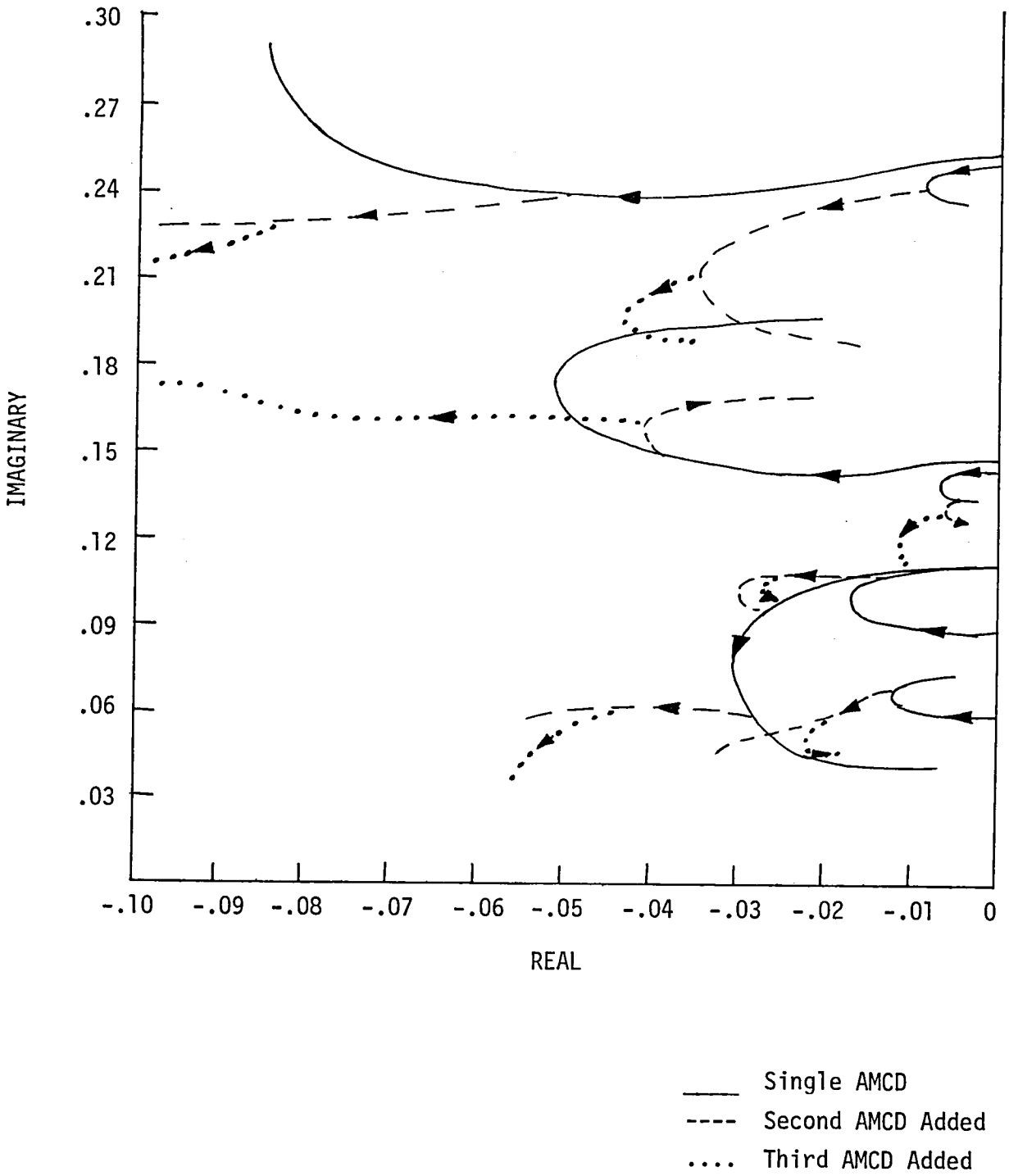

Figure 3.- Secondary controller root loci

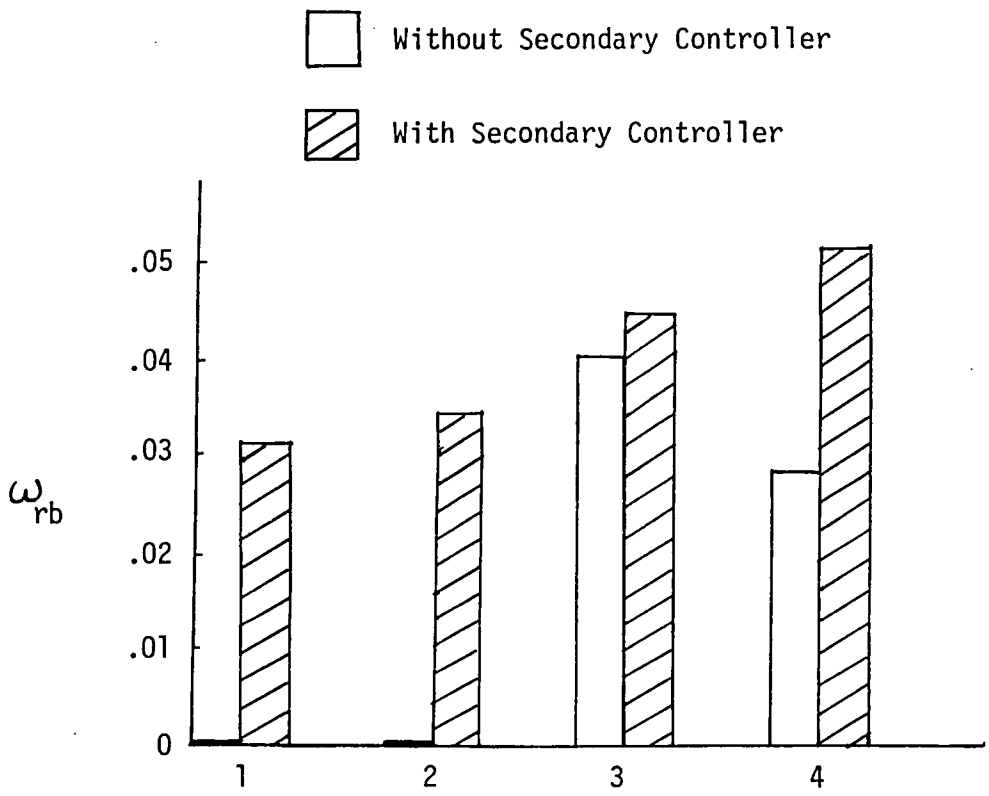

Highest Closed-Loop Rigid-Body Frequency

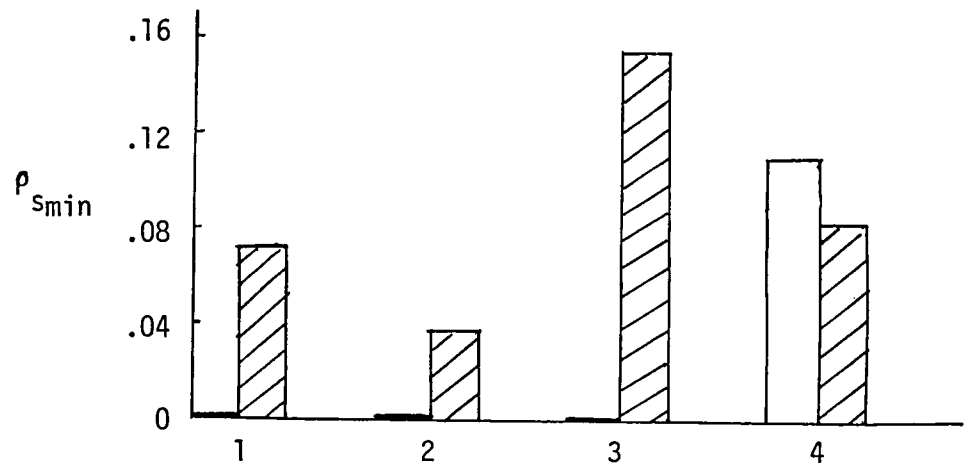

Lowest Closed-Loop Structural Damping Ratio

Case 1. Non-colocated primary actuator (single)/sensor - truncation method

Case 2. As above, but modified truncation method

Case 3. Colocated primary actuator (single)/sensor

Case 4. Colocated primary actuators (three)/sensors

Figure 4.- Numerical results for primary attitude controller

1. Report No.	2. Government Accession No.	3. Recipient's Catalog No.
NASA CR-165717		

4. Title and Subtitle	5. Report Date
A Controller Design Approach for Large Flexible Space Structures	May 1981
	6. Performing Organization Code
7. Author(s)	8. Performing Organization Report No.
S. M. Joshi	
9. Performing Organization Name and Address	10. Work Unit No.
Vigyan Research Associates, Inc. 28 Research Drive Hampton, VA 23666	11. Contract or Grant No. NAS1-16126
12. Sponsoring Agency Name and Address	13. Type of Report and Period Covered Contractor Report 2/22/80-4/30/81
National Aeronautics and Space Administration Washington, DC 20546	14. Sponsoring Agency Code

15. Supplementary Notes

Langley Technical Monitor: Harold A. Hamer
Final Report

16. Abstract

A controller design approach for large space structures is presented, which consists of a primary attitude controller and a secondary or damping enhancement controller. The secondary controller, which uses several Annular Momentum Control Device (AMCD's), is shown to make the closed-loop system asymptotically stable under relatively simple conditions. The primary controller using torque actuators (or AMCD's) and colocated attitude and rate sensors is shown to be stable. It is shown that the same AMCD's can be used for simultaneous actuation of primary and secondary controllers. Numerical results are obtained for a large, thin, completely free plate model.

17. Key Words (Suggested by Author(s))	18. Distribution Statement
Control of large space structures Annular Momentum Control Device (AMCD)	Unclassified - Unlimited Subject Category 18

19. Security Classif. (of this report)	20. Security Classif. (of this page)	21. No. of Pages	22. Price*
Unclassified	Unclassified	51	A04

For sale by the National Technical Information Service, Springfield, Virginia 22161